IIETA International Information and Engineering Technology Association
Advancing the World of Information and Engineering

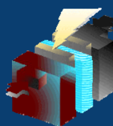

Journal of New Materials for Electrochemical Systems
Vol. 26, No.2, April 2023, pp.101-106
Journal homepage: http://iieta.org/journals/jnmes

Thickness, Structure, Composition and Optical Properties of Electrochemically Grown Iron Selenide and Iron Diselenide Thin Films

S. Thanikaikarasan[1*], R. Perumal[2], E Thanikaivelan[3], Tansir Ahamad[4], Saad M Alshehri[4]

[1]Department of Physical Sciences, Saveetha School of Engineering, Saveetha Institute of Medical and Technical Sciences, Chennai - 602 105, Tamil Nadu, India.

[2]Deparment of Materials Physics, Saveetha School of Engineering, Saveetha Institute of Medical and Technical Sciences,Chennai - 602 105, Tamil Nadu, India.

[3]Department of Physics, Vel Tech Multi Tech Dr. Rangarajan Dr. Sakunthala Engineering College, Avadi, Chennai- 600062, Tamil Nadu, India.

[4]Department of Chemistry, College of Science, King Saud University, Riyadh -11451, Kingdome of Saudi Arabia.

Corresponding Author Email: s_thanikai@rediffmail.com

https://doi.org/10.14447/jnmes.v26i2.a01

Received: September 22, 2022
Accepted: March 15, 2023

Keywords:
Band gap, Electrodeposition, Ferroselite, , Thin films, wurtzite

ABSTRACT

Iron chalcogenides attracted researchers in several applications due to its prominent characteristics viz., band gap, crystalline nature and composition along with its chemical and optical properties. The main intention of the present work is to determine the modified features of iron selenide and iron diselenide thin film growth by simple electrodeposition technique. Thin films of iron selenide and iron diselenide are deposited on transparent nature conducting substrates. Structural properties reported that the deposited films found to be polycrystalline in nature. The structural parameters such as crystallite size, strain, dislocation density and stacking fault probability were determined. Microscopic images showed that deposited films have well defined morphology with nearly stoichiometry. The band gap value of the deposited films found to be around 1.21 eV. The parameters refractive index, extinction coefficient of the deposited films are estimated.

1. INTRODUCTION

Chalcogenides of iron attracted many researchers due to its extensive applications in numerous fields [1-2] viz., photovoltaic [3], semiconductors [4], superconducting and sensing devices [5]. There is an existence of several non-stoichiometric, stoichiometric phases of iron selenide compounds such as Fe_3Se_4, Fe_3Se_7, $FeSe_2$ and FeSe**.** The stoichiometric phases of alloys $FeSe_2$, FeSe are well known semimagnetic semiconductors received much attention in magnetic and spintronic applications [6].The alloys of FeSe and $FeSe_2$ found to be crystallized in hexagonal structure and orthorhombic structure. The percentage of elemental Se is in the range between 48 and 56 %, determine the properties of magnetic materials such as ferromagnetic, paramagnetic and diamagnetic [6]. Thin films of FeSe and $FeSe_2$ found to be p-type semiconductor with an energy gap value in the range between 1.23 and 1.08 eV which make them interesting for its applications in superconductors, photovoltaic and optoelectronics devices [7-8]. Thin films of FeSe found to be crystallized in the hexagonal structure (PDF-75-0608, JCPDS ICDD 2003) with lattice constants (a = 3.61 Å ; c = 5.87 Å) at lower temperature whereas $FeSe_2$ thin films are crystallized in orthorhombic structure with lattice constants (a = 4.801 Å; b = 5.776 Å; c = 3.585 Å). Several physical and chemical techniques employed to prepare FeSe and $FeSe_2$ thin films such as thermal evaporation, sputtering, chemical bath deposition, spray pyrolysis and so on [9-13]. The technique of electrochemical deposition has been evidenced as a powerful ability to control the crystallization of iron selenide, iron diselenide thin films and it presents a simple, economical, cost effective, less time consuming as well as adjustment of the deposition parameters with composition of electrolytic bath along with its film stoichiometry [14-16].

In the present report, thin films of FeSe and $FeSe_2$ were deposited on transparent nature conducting ITO substrates by simple, low cost electrodeposition technique. Structural properties of the deposited films determined using X-ray diffraction. The characterization techniques viz., scanning electron microscopy, Energy dispersive X-ray analysis and UV-visible-NIR spectroscopy have been carried out to determine the surface morphology, film composition and optical properties of the deposited films.

2.1. Electrodeposition of FeSe and $FeSe_2$ thin films

The source of chemicals $FeSO_4$ $7H_2O$, SeO_2, dilute H_2SO_4 used were of AR grade reagents (E-Merck). The potentiostatic deposition of FeSe and $FeSe_2$ was carried out using Potentiostat/Galvanostat (SP 50, Bio Logic, France) with three electrode cell arrangement consists of ITO substrate, Graphite rod and Saturated Calomel Electrode (SCE) as cathode, anode and reference electrodes, respectively. The working electrode with area of cross section 2 x 1.5 cm^2 were cleaned in acetone with ultrasonic bath for 15 minutes. Thereafter, they were well cleaned with running distilled water for the duration of 10 minutes. Finally the substrates were subjected to the process of drying in air for 20 minutes. The electrolytic bath consists of 0.02 M $FeSO_4$, 0.002 M SeO_2 for FeSe, whereas 0.02 M $FeSO_4$, 0.02 M SeO_2 for $FeSe_2$, respectively.The films deposited at bath temperature below 50°C, the current density is found to be lower reduces the release of ions with poor adherence nature

to the substrate. If the temperature was increased above 50°C, the rate of release of ions was found be to be higher produces films with well adherence nature to the substrate. The increase of bath temperature above 80°C the value of current density found to be lower resulted peel off nature of film from the substrate. As a result, the bath temperature was maintained in the range between 50 and 80°C. The pH value of the electrolytic bath was initially at 4.0 ± 0.1, thereafter reduced to 2.5 ± 0.1, by the addition of an adjustable amount of dilute H_2SO_4 to the electrolytic bath. The optimized value of pH was maintained in the range between 2.0 and 2.5 ± 0.1 to obtain films with good quality. The time of deposition was found to be in the range between 5 and 50 minutes. Also, the deposition potential was fixed in the range between -500 and -1300 mV versus SCE for the deposited films of FeSe and $FeSe_2$.

2.2. Characterization

The method of weight difference was used to find out thickness value of the deposited films. The electrochemically grown FeSe and $FeSe_2$ thin films were subjected to the characterization of X-ray diffraction using Phillips diffractometer at 40 kV and 300 mA within the diffraction angle in between 20 and 80 degree have CuKα target (λ = 1.5406Å). The morphological feature along with composition was analyzed using an Energy dispersive X-ray analysis set up attached with JEOL JSM 840 Scanning electron microscope. The technique of UV-Visible– NIR spectroscopy was carried out to determine the percentage of absorbance and transmittance nature of the deposited films using Shimadzu UV-Visible NIR spectrometer.

3. Results and Discussion

3.1. Growth Kinetics

The stoichiometric growth of FeSe and $FeSe_2$ phase takes place according to the following Eq's (1) to (4). The decomposition of Fe^{2+} from compound $FeSO_4\,7H_2O$ takes place according to Eq (1), whereas the decomposition of Se^{2-} takes place according to Eq.(2)

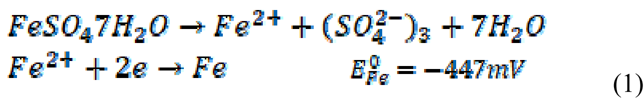

$$FeSO_4 7H_2O \rightarrow Fe^{2+} + (SO_4^{2-})_3 + 7H_2O$$
$$Fe^{2+} + 2e \rightarrow Fe \qquad E^0_{Fe} = -447mV \qquad (1)$$
$$E_{Fe} = E^0_{Fe} - \left[\frac{RT}{2F}\right] ln \left[\frac{a_{Fe}}{a^{2+}_{Fe}}\right]$$

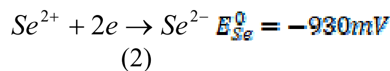

$$Se^{2+} + 2e \rightarrow Se^{2-} \quad E^0_{Se} = -930mV \qquad (2)$$
$$E_{Se} = E^0_{Se} - \left[\frac{RT}{2F}\right] ln \left[\frac{a_{Se}}{a_{Se^{2-}}}\right] + \left[\frac{RT}{4F}\right] ln(\,a^{+}_{H})^4$$

The formation of FeSe and $FeSe_2$ takes place according to the following Eq's (3) & (4)

$$Fe^{2+} + Se^{2-} + 4e \rightarrow FeSe \qquad (3)$$

$$Fe^{2+} + 2Se^{2-} + 4e \rightarrow FeSe_2 \qquad (4)$$

The growth of the deposited FeSe and $FeSe_2$ thin film layers on ITO substrates which have been adjusted mainly by film thickness and surface morphology. The significant parameters such as current density, solution pH, bath temperature and electrolyte concentration plays an essential role to find out thickness value of the deposited films [17-18].Thickness of the deposited films was determined from the bulk density, weight difference in which the film deposited on substrate before and after certain intervals of time. Thickness of the deposited films was calculated by using the following Eq.(5) [14]

$$t = \frac{m}{A\rho} \qquad (5)$$

Thickness of the deposited FeSe and $FeSe_2$ thin films was found to be in the range between 1250 and 1400 nm (Table 1).

3.2 . Structural Properties

X ray diffraction pattern has been taken out to identify the crystalline nature and phases of the deposited films. XRD pattern recorded for FeSe thin films deposited on ITO substrate at optimized condition is shown in Figure 1a. It is noted that the deposited films found to exhibit hexagonal structure.The identification of peaks in the diffractogram found at 2θ values 28.49, 30.40, 42.20, 50.51, 55.35, 60.15, 67.93 and 78.26, corresponding to the lattice planes (100), (002), (102), (110), (103), (112), (202) and (203) for hexagonal FeSe, respectively[19]. The orientation of the deposited film found to be (002) along the substrate. XRD pattern recorded for $FeSe_2$ thin films deposited on ITO substrate is shown in Figure 1b. The diffraction peaks of $FeSe_2$ found at 2θ values 24.06, 31.07, 34.77, 36.22, 40.20, 44.42, 48.14, 49.32, 54.09 and 59.53 correspondingto the lattice planes (1 1 0), (1 0 1), (1 1 1), (1 2 0), (2 1 0), (1 2 1), (2 1 1), (2 2 0), (0 3 1) and (3 1 0), respectively [20]. The deposited films found to exhibit most prominent reflection along (120) plane along the surface. The value of lattice constants "a", "c" for hexagonal phase FeSe and "a", "b", "c" for orthorhombic phase of $FeSe_2$ are estimated using the following Eq.'s(6) & (7) [15,18]

$$\frac{1}{d^2} = \frac{4}{3}\left[\frac{h^2 + hk + l^2}{a^2}\right] + \frac{l^2}{c^2} \qquad (6)$$

$$\frac{1}{d^2} = \frac{h^2}{a^2} + \frac{k^2}{b^2} + \frac{l^2}{c^2} \qquad (7)$$

The value of crystallite size for the deposited FeSe and $FeSe_2$ thin films was calculated using Debye Scherrer formula [21].

$$D = \frac{0.9\lambda}{\beta \cos\theta} \qquad (8)$$

where β is the Full Width at Half Maximum of the peak position in radian, λ is the wavelength of CuK_α target used (λ= 1.540 Å), θ is Bragg diffraction angle at peak position in degree.The films deposited at lower temperature around 80°C found to be polycrystalline nature when compared with films obtained by other techniques viz., thermal evaporation, vaccum evaporation, sputtering, spray pyrolysis and so on.

(

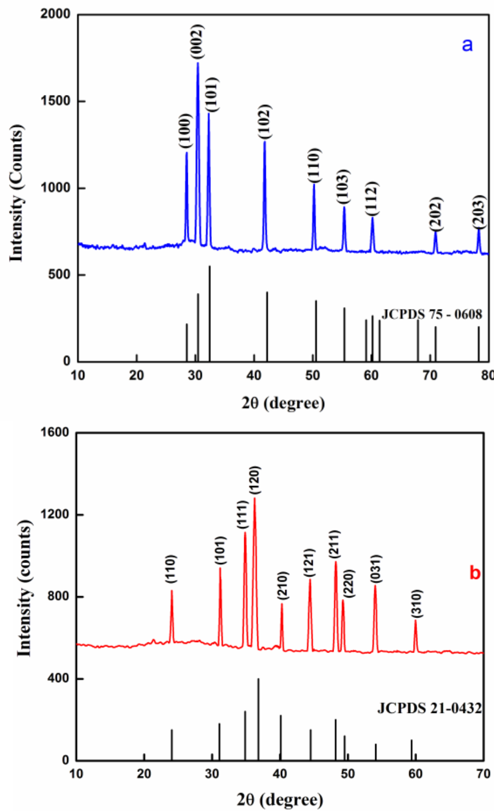

Figure 1a,b XRD pattern of electrodposited FeSe and $FeSe_2$ thin films

XRD technique appears to be attractive to find out the value ofstrain, dislocation density and stacking fault probability of the deposited films. Strain is defined as the restricted force which can be acts along the substrate surface.The method of variance analysis given by the method Mitra has been used to estimate the value of strain present in the deposited films [22]. The rms microstrain present in the deposited films is calculated using the following Eq.(9). The number of dislocation lines present in the deposited films is termed as dislocation density [23].The value of dislocation density and stacking fault probability were determined using the following Eq.(10).

$$W_{2\theta} = \left[\frac{\lambda a}{(2\pi^{2} D \cos\theta)}\right] + 4\tan^{2}\theta < e^{2} > \quad (9)$$

$$\rho = \frac{3.46 < e^{2} >^{1/2}}{dD} \quad (10)$$

where $<e^2>$ the microstrain, ρ is the dislocation density. The stacking fault probability (α) is the fraction of layers undergoing stacking sequence faults in a given crystal and hence one fault is expected to be found in (1/ α) layers [24]. The presence of stacking faults gives rise to a shift in peak position of different reflections with respect to ideal position of a fault-free well-annealed sample and hence to evaluate the structural parameters. The values of stacking fault probability estimated for the deposited films using the following Eq.( ).

$$\alpha = \left[\frac{2\pi^{2}}{45\sqrt{3}}\right]\left[\frac{\Delta(2\theta)}{\tan\theta}\right] \quad (11)$$

The estimated value of lattice parameters such as lattice constants, crystallite size, strain and dislocation density are given in Table 1.

3.3. Surface morphology and film composition

Morphological view along with composition for the deposited iron selenide and iron diselenide thin films was analyzed using an Energy dispersive X-ray analysis set up attached with Scanning Electron Microscopy.The SEM image with EDX spectra of FeSe thin film deposited on ITO substrate is shown in Figure 2a,b. It is noted that the surface is found to be smooth with coverage of spherically shaped grains. The emission lines of Fe and Se are present in the investigated energy range denoted the formation of FeSe thin films. The atomic percentage (Fe:Se) value of FeSe thin films deposited on ITO substrate is found to be 52.27:48.04. Similarly, the uniform distribution of spherically shaped grains and the composition of the deposited layers of $FeSe_2$ with film composition (65.38:34.17) was analyzed and shown in Figure 3a,b. The atomic percentage of the deposited $FeSe_2$ layers was found to be nearly stoichiometric nature of the deposited films.The estimated value of elemental percentage for FeSe and $FeSe_2$ thin films are given in Table 1 (see end of article).

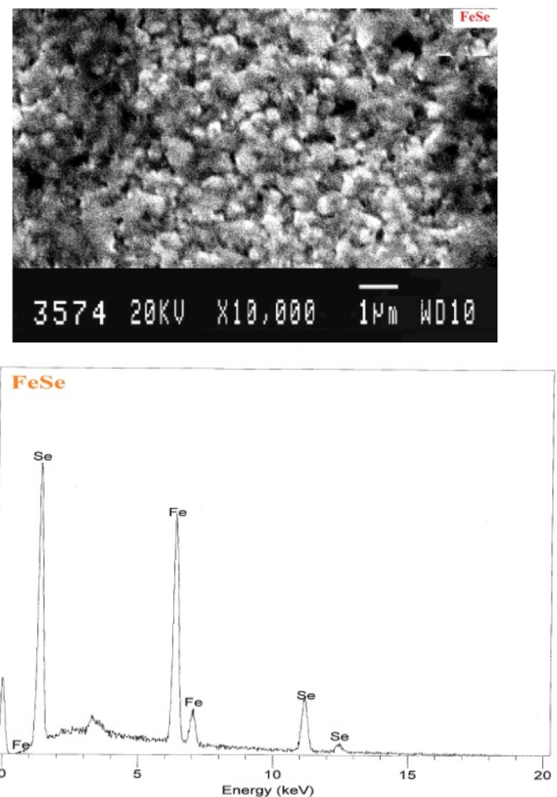

Figure 2a,b SEM image and EDX spectrum of FeSe thin films

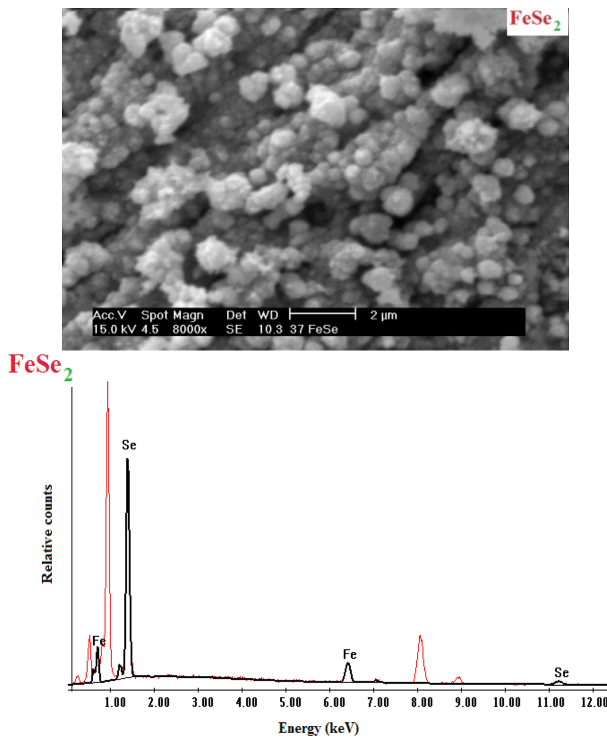

Figure 3a,b SEM image and EDX spectrum of $FeSe_2$ thin films

3.4. Optical Properties

The knowledge of band structure with the value of energy gap in eV is the determination of transmittance, absorption and reflectance measurement of the deposited FeSe and $FeSe_2$ films. In the present study, the percentage of optical absorbance and transmittance was recorded within the wavelength range in between 350 and 1100 nm. The nature of transition present in the deposited films is determined by using the following Eq.(11)[16,17]

$$\alpha = \frac{A(h\vartheta - E_g)^n}{h\vartheta} \quad (11)$$

where (hν) is the photon energy in eV, Eg is the band gap energy in eV, α is the absorption coefficient in cm^{-1}. The value of n=1/2 indicated that the direct transition of the deposited FeSe and $FeSe_2$ thin films.

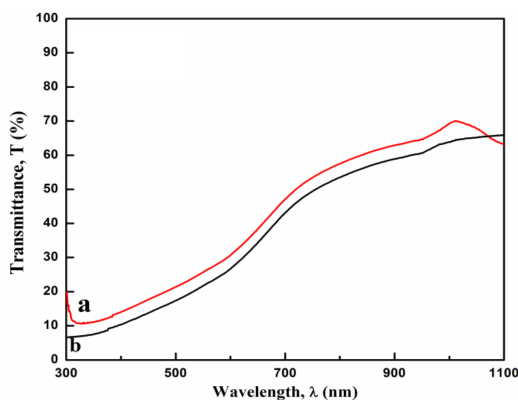

Figure 4a,b. Transmittance percentage of FeSe and $FeSe_2$ thin films deposited on ITO substrate

Figure 4a,b shows the percentage of transmittance for FeSe and $FeSe_2$ thin films deposited on ITO substrate. It is noted that the percentage of transmittance is found to be maximum at 950 and 1099 nm. The value of maximum transmittance for the deposited film is found to be is in the range between 60 and 70. The presence of maximum transmittance in the range between 960 and 1050 nm related to the transportation of electron from the valence band (VB) to the conduction band (CB) of the deposited films. Plot of (hν) versus $(\alpha h\nu)^2$ for FeSe and $FeSe_2$ thin films deposited on ITO substrate is shown in Figure 5a,b. The linear portion of the plot to the X-axis (hν) gives band gap value of the deposited films. The deposited films found to exhibit energy gap value in between 1.04 and 1.24 eV for FeSe and $FeSe_2$ which must be closer to the value reported earlier [15,18]

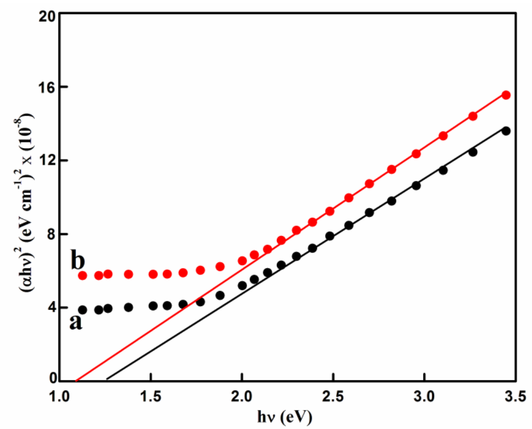

Figure 5a,b Taucs plot for FeSe and $FeSe_2$ thin films deposited on ITO substrate

Refractive index “n” is one of the basic properties of semiconductors and it is defined as the ratio of sine angle of incidence to sine angle of refraction. The value of refractive index and extinction coefficient of the deposited films has been calculated using the following relation’s.

$$n = \left(\frac{1+R}{1-R}\right) - \sqrt{\frac{4R}{1-R}} - k^2 \quad (12)$$

$$k = \frac{\alpha\lambda}{4\pi} \quad (13)$$

where n is the refractive index, k is the extinction coefficient, λ is the wavelength in nm. Variation of refractive index “n” with wavelength “λ” for FeSe and $FeSe_2$ thin films is shown in Figure 6. Also the variation of extinction coefficient with wavelength for FeSe and $FeSe_2$ thin films deposited on ITO substrate is shown in Figure 7. The decrease in value of “k” with increase in the value of “λ” displays that the fraction of light lost due to scattering and decrease in the ratio of absorption [17]. After these wavelengths, the curves exhibited a peak due to absorption, and then these values tend to remain constant.

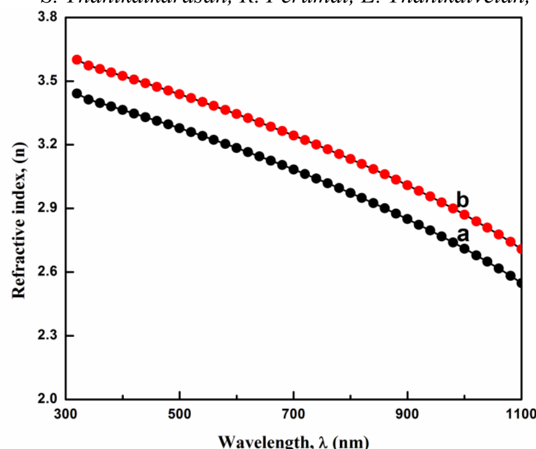

Figure 6a,b Variation of refractive index (n) with wavelength (λ) for FeSe and $FeSe_2$ thin films deposited on ITO substrate

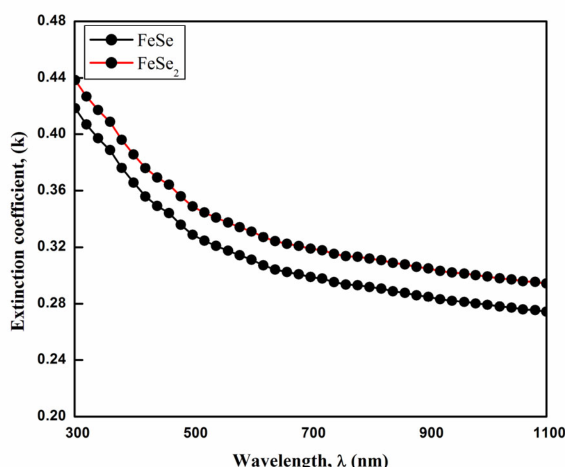

Figure 7a,b Variation of extinction coefficient (k) with wavelength (λ) for FeSe and $FeSe_2$ thin films deposited on ITO substrate

4. CONCLUSIONS

Thin films of FeSe and $FeSe_2$ were successfully deposited on ITO substrates by simple low temperature electrodeposition technique. Structural features showed that the deposited films found to be polycrystalline nature with hexagonal and orthorhombic structure for FeSe and $FeSe_2$. The value of structural parameters such as crystallite size, strain, dislocation density were determined. Morphological feature showed that the films with smooth surface and well defined stoichiometry. Optical properties denoted that the band gap value was found to be 1.21 and 1.08 eV for FeSe and $FeSe_2$. The parameters such as refractive index, extinction coefficient were estimated for the deposited films.

ACKNOWLEDGEMENT

The authors extend their sincere appreciation to the Researchers Supporting Project Number (RSP2023R6), King Saud University, Riyadh, Saudi Arabia for funding this research.

REFERENCES

[1].Ashok U Ubale, Naina R Welekar, AmrutaV Mitkari (2014) Effect of annealing on physical properties of CBD synthesized nanocrystalline FeSe thin films Mater. Sci. Semicond. Process. 27, 280 – 287 (https://doi.org/10.1016/j.mssp.2014.06.035)

[2].Ouertani B., Ouerfelli J., Saadoun, Bessa B.,M., Ezzaouia H., Bernedè J.C., (2005) Transformation of amorphous iron oxide thin films pre deposited by spray pyrolysis into a single FeSe2 phase by selenisation Sol. Energy Mater. Sol. Cells 87,501- 511. https://doi.org/10.1016/j.solmat.2004.07.036

[3]. Mitzi D.B., Yuan M., Liu W., Kellock A.J., S.J.Chey, Deline V., Schrott A.G., (2008) A High-Efficiency Solution-Deposited Thin-Film Photovoltaic Devices Adv .Mater. 765,3657–3662. https://doi.org/10.1002/adma.200800555C

[4] Tomasz Dietl (2002) Ferromagnetic Semiconductors Semicond. Sci. Technol 17, 377- 392. https://doi.org/10.1088/0268-1242/17/4/310

[5] Schöning M.J., Kloock J.P., (2007) About 20 Years of Silicon-Based Thin-Film Sensors with Chalcogenide Glass Materials for Heavy Metal Analysis: Technological Aspects of Fabrication and Miniaturization J Electroanal. Chem. 9 2029–2038. https://doi.org/10.1002/elan.200703955

[6].XWu,Z.Zhang,J.Zhang,Z.Ju,B.Li,C.Shan,D.Zhao,B.Yao ,D.Shen, (2008) Growth of FeSe on general substrates by metal-organic chemical vapor deposition and the application in magnet tunnel junction devices Thin Solid Films 516, 6116–6119. https://doi.org/10.1016/j.tsf.2007.11.012

[7] X. Wu, Z.Zhang, J.Zhang, B.Li, Z.Ju, Y.Lu, B.Li, D.Shen, J. Appl. Phys.103 (2008),113501-113501-113506.

[8] A.Mars , H.Essaidi, J.Ouerfelli (2015) Optical and electrical measurement of FeSe2 thin films obtained at low temperature Mater. Sci. Semicon. Proc. 40 319–324. https://doi.org/10.1016/j.mssp.2015.06.030

[9] Ubale A., Sakhare Y., Bombatkar S., (2013) Influence of the complexing agent (Na2-EDTA) on the structural, morphological, electrical and optical properties of chemically deposited FeSe thin films, Mater. Res. Bull.48,3564–3571. https://doi.org/10.1016/j.materresbull.2013.05.064

[10] Rong Jin, Xiaoyan Pu KeZhao, Min Zhang, (2016) Structural and photovoltaic properties of FeSe2 films prepared by radio frequency magnetron sputtering Fanggong Cai, Xinsheng Yang,Hern Kim, Yong Zhao, Mater. Lett. 179 179 - 181. https://doi.org/10.1016/j.matlet.2016.05.087

[11] Ubale A., Sakhare Y., Bombatkar S., (2013) Influence of the complexing agent (Na_2-EDTA) on the structural, morphological, electrical and optical properties of chemically deposited FeSe thin films, Mater. Res. Bull. 48, 3564-3571. https://doi.org/10.1016/j.materresbull.2013.05.064

[12] Chen T.K., Luo J.Y., Ke C.T., Chang H.H., Huang T.W., Yeh K.W., C.C. Chang,P.C. Hsu, C.T. Wu, M.J. Wang, M.K. Wu, (2010) Low-temperature fabrication of superconducting FeSe thin films by pulsed laser deposition Thin Solid Films 519,1540 -1545. https://doi.org/10.1016/j.tsf.2010.06.002

[13] Ubale A, Sakhare Y, J. Phys. Chem. Solids (2013) Effect of substrate temperature on optical, structural and electrical properties of FeSe thin films deposited by spray pyrolysis technique, J Phys. Chem. Solids, 74, 1464. https://doi.org/10.1016/j.jpcs.2013.05.006

[14] S.Thanikaikarasan, (2021) Role of electrolyte concentration on growth kinetics, film thickness, structural, compositional and optical properties of cadmoselite thin films through electrochemical route, J Alloys Compd 885, 160963 https://doi.org/10.1016/j.jallcom.2021.160963

[15] Thanikaikarasan S., Mahalingam T., Sundaram K., Kathalingam A., Yong Deak Kim, Taekyu Kim, (2009) Growth and characterization of electrosynthesized iron selenide thin films Vacuum, 83,1066-1072. https://doi.org/10.1016/j.vacuum.2009.01.004

[16] Jeyakumar P., Thanikaikarasan S., Natarajan B., (2017) J Mater. Sci- Mater. El 28 2538–2544 https://doi.org/10.1007/s10854-016-5828-z

[17] Bharathi B., Thanikaikarasan S, Pratap Kollu, Chandrasekar P V , Sankaranarayanan, K. Sahaya Shajan X. , J Mater. Sci- Mater. El. 25 (2014) 5338-5344. https://doi.org/10.1007/s10854-014-2310-7

[18] Thanikaikarasan S., Mahalingam T., (2012) Influence of solution pH in electrodeposited iron diselenide thin films mpd. J Alloys Co., 511, 115-122. https://doi.org/10.1016/j.jallcom.2011.09.003

[19] Joined Council for Powder Diffracted System International Centre for Diffraction Data, Pennsylvenia, USA, 2003. File No.75-0608.

[20] Joined Council for Powder Diffracted System International Centre for Diffraction Data, Pennsylvenia, USA, 2003. File No.21-0432

[21] Cullity BD, Stock SR. Elements of X-ray diffraction. 3rd ed.London: Pearson Publishers; 2001.

[22] Mitra G B , Misra N K (1966). Background errors in X-ray diffraction parameters. Brit J Appl. Phys 17 (10) 1319-1328. doi.org/10.1088/0508-3443/17/10/310

[23] Williamson G K, Smallman R E (1956). Dislocation densities in some annealed and cold-worked metals from measurements on the X-ray debye-scherrer spectrum. Philos Mag. 1:34-46.doi.org/10.1080 /14786435608238074

Table 1. Structural and optical parameters estimated for the deposited FeSe and $FeSe_2$ thin films.

Sample	**Crystal lite size, P (nm)**	**Rms strain, $<e^{1/2}>$ (10^{-4}) (line^{-2}metre^{-4})**	**Dislocation density, (ρ) (10^{14}) lines metre^{-2}**	**Lattice constant (Å)**			**Atomic (%)**		**Band gap, E_g (eV)**	**n**	**K**
				a	b	c	Fe	Se			
FeSe	**42.17**	**9.52**	**5.63**	**3.321**	**--**	**5.431**	**52.24**	**47.76**	**1.26**	**3.17**	**0.26**
$FeSe_2$	**45.54**	**7.82**	**4.85**	**5.721**	**5.718**	**3.520**	**65.93**	**34.07**	**1.07**	**2.37**	**0.75**